Ain Shams Engineering Journal xxx (xxxx) xxx

Contents lists available at ScienceDirect

Ain Shams Engineering Journal

journal homepage: www.sciencedirect.com

Civil Engineering

The study of properties and behavior of self compacting concrete containing Electric Arc Furnace Slag (EAFS) as aggregate

Amaia Santamaría [a,1], Vanesa Ortega-López [b,*], Marta Skaf [c,2], José Antonio Chica [d,3], Juan Manuel Manso [b,2]

[a] Department of Mechanical Engineering, University of the Basque Country, UPV/EHU, Spain
[b] Department of Civil Engineering, University of Burgos, Spain
[c] Department of Construction, University of Burgos, Spain
[d] Sustainable Construction Division, Fundación Tecnalia Research & Innovation, Spain

ARTICLE INFO

Article history:
Received 12 July 2019
Revised 2 October 2019
Accepted 3 October 2019
Available online xxxx

Keywords:
Electric arc furnace slag
Self-compacting concrete
In-fresh properties
Long-term hardened properties
Sustained load testing

ABSTRACT

Electric Arc Furnace Slag (EAFS) can be efficiently reused as aggregate in the production of high-volume batches of hydraulic concrete mixes that show interesting properties in both the fresh and the hardened state. Mixtures containing EAFS aggregate in proportions of nearly 50% by volume are prepared for use as pumpable and self-compacting mixes with consistency classes of S4 and SF2, respectively. Characterization of the mixtures is presented, examining practical aspects such as thixotropy, segregation in the fresh state (under 6%), and mechanical and microstructural evolution in the hardened state. The results yielded compressive strengths of approximately 60 MPa and elastic moduli of 38 GPa after one year. Finally, real-scale flexural elements are cast and subjected to sustained loading tests of moderate intensity. Long-term deflection values were approximately 50% (pumpable mixes) and less than 40% (self-compacting mixes) of the maximum admissible values specified in current standards.

1. Introduction

We live in a consumer society that has for decades been manufacturing short-lived disposable products that generate large volumes of waste. As the concept of sustainability gains ground, many industrial sectors have started to express an interest in sustainable practice linked to the future of the planet [1–3]. One of the main issues surrounding global sustainability is how to limit carbon emissions through the reuse of industrial by-products.

Many researchers have focused their studies on steelmaking slags [4–9]. The main research topics have specifically focused on the use of Electric Arc Furnace Slag (EAFS) include bedding materials for highways [10–14], bituminous mixes for pavement courses [15–22], and hydraulic binder mixes for monolithic elements [23–32]. Its use is also occasionally mentioned in the context of water depuration, energy storage, and abrasion-resistant layers

The physical and chemical properties of EAFS [33–36] aggregates are advantageous in hydraulic concrete mixes, producing concretes with improved hardened properties [37–43]. They are in many cases of similar durability to conventional concretes manufactured with natural aggregates [42,44–49]. Certain drawbacks have been encountered with the use of EAFS concretes, among which its higher density, tolerable in some applications for foundations, but detrimental in overhanging elements. Likewise, the poorer workability of in-fresh mixes may be mentioned that is advantageous in roller-compacted concrete, but detrimental in pumpable concrete. As ever, the challenge in terms of engineering good materials is the mitigation of their disadvantages and the enhancement of their advantageous qualities.

Encouraging research results have been published on EAFS mass concrete and its promising behavior at laboratory scale has convinced some (albeit very few) entities to apply these aggregates to real construction works. In 2008, the large foundation slab and

* Corresponding author at: Civil Engineering Department, EPS University of Burgos, Calle Villadiego s/n, 09001 Burgos, Spain.
E-mail addresses: amaia.santamaria@ehu.es (A. Santamaría), vortega@ubu.es (V. Ortega-López), mskaf@ubu.es (M. Skaf), joseantonio.chica@tecnalia.com (J.A. Chica), jmmanso@ubu.es (J.M. Manso).
[1] Address: Escuela de Ingeniería de Bilbao, I (bloque B) – UPV/EHU, Plaza Ingeniero Torres Quevedo, 1, 48013 Bilbao, Spain.
[2] Address: Escuela Politécnica Superior, Calle Villadiego s/n, 09001 Burgos, Spain.
[3] Address: TECNALIA, Parque Tecnológico de Bizkaia C/Geldo, Edificio 700, E-48160 Derio, Bizkaia, Spain.

Peer review under responsibility of Ain Shams University.

ELSEVIER Production and hosting by Elsevier

https://doi.org/10.1016/j.asej.2019.10.001
2090-4479/

basement walls of the KUBIK research building (Fig. 1a) at Tecnalia (Bilbao – Spain) were manufactured with EAF slag concrete. In 2015, the Port of Bilbao Authority (Bilbao Harbor – Spain) used EAFS concrete to manufacture heavy marine blocks for the "Punta Lucero" dock walls and to build the new "Punta Sollana" dock (see Fig. 1(b and c)) [50], both of which are exposed to aggressive marine environments. As previously mentioned, in these specialist applications, where the concrete is cast by gravity and where the structural performance of the application is directly related to its weight, the use of steel slag as aggregate was advantageous, due to its higher density and high resistance to chloride ions present in seawater and coastal environments.

Divulgation of this type of EAFS concrete and the extension of its use to construction components will as always depend on a demonstrable suitability and affordability in practical applications [51]. In this paper, both the in-fresh and the in-hardened behaviors of medium-strength concrete mixtures (compressive strength of 30–50 MPa at 28-days) containing EAFS coarse aggregate are characterized, in the particular context of manufacturing large batches of concrete (over one cubic meter) using industrial mixing machines. In recent publications [52–54], the authors successfully manufactured medium–strength self-compacting concrete with EAF slag coarse aggregate in "experimental size" batches (less than fifty liters), using a mix design that differed from the classical designs of concrete mixes made with conventional aggregates. The engineering challenges of pouring large rather than small batches into molds have been analyzed and addressed by various authors [55,56].

Very few studies along the same lines as the present paper have been reported. Worth mentioning are the pioneering papers published over the last decade in South Korea (Sang-Woo, Yong-Jun, Kil-Hee and altera) studying the behavior of flexural (2.6–3 m span) elements manufactured with EAFS as aggregate [57–60]. Likewise, Pellegrino and Faleschini [61–64] studied flexural and shear failure of 2 m long EAFS-RC (reinforced concrete) elements, showing that the ultimate flexural and shear stress was higher in beams manufactured with slag concrete than in beams with conventional concrete aggregate. The use of self-compacting mixtures of sustainable EAFS concrete in beam applications represents the original contribution of this paper.

2. Materials and proportions

2.1. Water, cement and natural aggregates

Mix water containing no compounds with adverse effects on hydraulic binder mixes was taken from the urban mains supply of the city of Burgos-Spain.

Two types of cement were used in the present article; firstly, a classical Portland cement type-I 52.5 R; secondly, a commercial Portland cement type-IV/B-V 32.5-N; both certified by the EN 197-1 standard [65]. The type-I cement included 90% Portland clinker with no specifications concerning the usual properties (hydration heat, sulfate resistance, and high early strength), 5% calcium carbonate fines, and 5% gypsum by weight, with a specific gravity of 3.15 Mg/m^3. The type-IV/B-V cement included 5% calcite powder fines, 40% fly ash type-I, 50% Portland clinker without special specifications, and 4% gypsum by weight, showing a specific gravity of 3 Mg/m^3.

The fine fraction (passing sieve N° 16, 1.18 mm mesh) of a natural limestone commonly used in northern Spain (calcite fraction >95%, Los Angeles loss in the interval 16–20%) was used with a fineness modulus of 1.5 units, specific gravity 2.65 Mg/m^3, and a gradation curve presented in Fig. 2. The main characteristics of this mineral fraction can be found in previous publications by the authors [23,52], which can be considered complementary to this study and that contain detailed information and analysis of the limestone fine fraction. It is however relevant to recall that its addition significantly improved the workability of the mixes, so that the consistency corresponds to self-compacting mixes, preventing segregation and compensating for the lack of fine particles in the 0–4 mm size fraction of EAFS.

2.2. EAF slag physical-chemical properties

Electric Arc Furnace slag (EAFS) in two size fractions (fine 0–4 mm and medium 4–12 mm), supplied by the company Hormor-Zestoa, was used in this research following processing, crushing, magnetic separation of metal, and three-months of weathering. The chemical composition and some physical properties are shown in Table 1; their gradations with a fineness modulus of 3.9 units for the fine fraction and 5.7 units for the medium-coarse fraction are shown in Fig. 2.

Perhaps the main characteristics of EAFS aggregate (in the form of fine and medium fraction gravel sizes), in comparison with the (non-homogeneous) set of natural aggregates for concrete, (mentioning only the main advantages of EAFS aggregate) are its roughness, angularity, toughness-strength-stiffness, abrasion resistance, density, and chemical basicity. Although they are all of interest, those of particular importance in the context of this article are included in Table 1, alongside a complete chemical analysis performed by energy -dispersive X-ray spectroscopy and identification of the main crystalline compounds with X-ray diffraction, to identify the type of EAFS and its content. Other authors have found similar characteristics in these types of EAFS slags [66].

Fig. 1. Kubik building foundation and basement walls (left); a concrete block from the Punta Lucero dock (center) and the Punta Sollana dock wall (right), both at Bilbao Harbor (Spain).

Please cite this article as: A. Santamaría, V. Ortega-López, M. Skaf et al., The study of properties and behavior of self compacting concrete containing Electric Arc Furnace Slag (EAFS) as aggregate, Ain Shams Engineering Journal, https://doi.org/10.1016/j.asej.2019.10.001

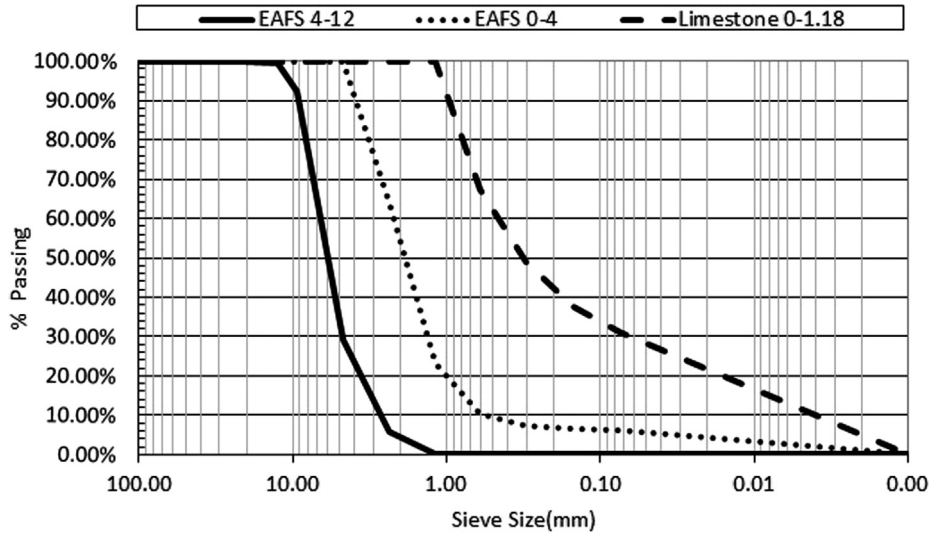

Fig. 2. Grading of concrete aggregates.

Table 1
Chemical composition and physical characteristics of EAFS.

Compounds	EAFS
Fe_2O_3 (%)	22.3
CaO (%)	32.9
Free CaO (%)	0.8
SiO_2 (%)	20.3
Al_2O_3 (%)	12.2
MgO (%)	3.0
MnO (%)	5.1
SO_3 (%)	0.42
Cr_2O_3 (%)	2.0
P_2O_5 (%)	0.5
TiO_2 (%)	0.8
Loss on ignition (%)	Gain
Water absorption (%)	1.12
Specific gravity (Mg/m^3)	3.42
Angularity number BS-812	Close to 11
Los Angeles loss (%)	12
X-ray diff. main compounds	Wüstite-GheleniteKirsteinite-Calcium olivine

2.3. Mix design

Four different concrete mixes were designed for this experimental campaign. They all contained EAFS slag as aggregate in the highest possible proportions, though they were all also designed to guarantee their applications in construction. In those mixes, EAFS constituted the totality of the coarse aggregate, and the larger-sized fraction (>1.2 mm) of the fine aggregate. The rest of the fine aggregate fraction (<1.2 mm) was a mix of small-size EAFS (see the grading of the EAFS fraction 0–4 in Fig. 2) and the above-mentioned fine fraction of limestone aggregate. The cement proportion (320–330 kg/m^3) and the w/c ratio (approx. 0.5 units) are standard values in large batches of concrete mixtures to obtain a medium compressive strength (>30 MPa after 28 days in moist-room-conserved samples). There are multiple combinations of cement content and different w/c ratios to perform mixtures. However, in this case, the aforementioned "conventional values" were chosen for these two variables, before approaching other types of variables and issues that may influence this aspect.

The first variable introduced in the design is the classification of the different cement types used for the manufacture of the sample specimens, type-I and type-IV/B (V) (EN 197-1 standard [65]. The former is the "reference" cement for industrial construction. The second is a more sustainable binder in which almost one half is another valuable industrial by-product (vitreous fly ash) produced by the energy industry (coal burning-combustion throughout the twentieth century), with abundant stockpiles around the world. The resultant mixes were labelled I-P (type-I cement and pumpable mix), I-SC (type-I cement and self-compacting mix), and, in a similar way, IV-P and IV-SC mixes. The binder variable was introduced to show the influence of the cement types on the in-fresh concrete properties. It also served to study the influence of the interaction between the mineral additions of cement (limestone filler, fly ash) and coarse EAF slag aggregate on the structure of the hardened concrete and its properties. Obviously, from a practical point of view, the use of the type-IV/B (V) cement enhanced both sustainability and economic cost, though it also yielded slightly inferior mechanical properties.

Workability was the second variable introduced in the design of the mixtures for both pumpable (P) and self-compacting (SC) mixes; it is widely known and accepted in the literature that an excessive presence of EAFS aggregate in concrete mixes detracts from their workability. Initially, a target slump of 200 mm in the Abrams cone test was set as the objective for the pumpable mixes, and a spread of 600 mm (of which 500 mm in over four seconds) for the self-compacting mixes, likewise using the Abram's cone test. These targets are not unusual in civil works for practical concrete engineering projects.

With regard to the slump tests, three factors can be outlined, considering that EAFS will form the only coarse mineral aggregate with gravel sizes between 1.2 and 12.5 mm. Firstly, the angularity of the slag particles is very high and the adherence between the slag particles and the cementitious matrix is also fairly high [52]; both factors mean that a high proportion of cementitious matrix is needed. Secondly, the external surface is markedly rough and resistant to abrasion and contact during the flow of concrete will be especially sharp and frictile between the EAFS particles; this effect has also to be mitigated by a suitable cementitious matrix. Thirdly, the EAFS particles are of a higher density than the conventional aggregates. The higher tendency to decantation-segregation due to gravity forces when suspended in fluid matrices is evident. Once again, the dynamic viscosity of the cementitious matrix, measured in terms of a Bingham plastic medium, must be suitable.

A suitable gradation of components and well-chosen chemical admixtures (water reducer, WR, and viscosity conditioner, VMA) must be employed, to obtain acceptable results in the operation of pouring large volumes of EAFS concrete into industrial molds

Please cite this article as: A. Santamaría, V. Ortega-López, M. Skaf et al., The study of properties and behavior of self compacting concrete containing Electric Arc Furnace Slag (EAFS) as aggregate, Ain Shams Engineering Journal, https://doi.org/10.1016/j.asej.2019.10.001

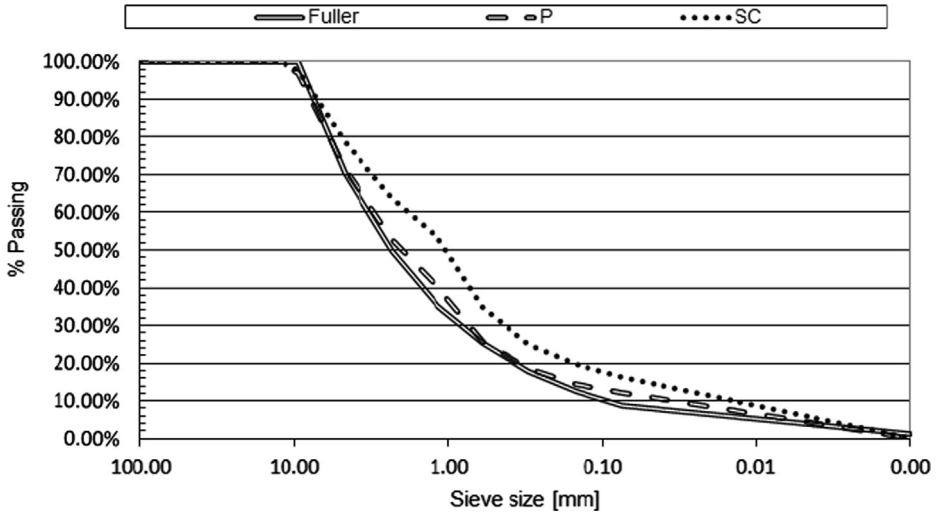

Fig. 3. In volume gradation of the mixes and Fuller's curve.

Table 2
Mix proportions in kg per cubic meter of concrete.

	IP	IVP	ISC	IVSC
Cement I	330		330	
Cement IV		320		320
Water	160	160	170	170
EAFS coarse (4–12 mm)	980	980	770	770
EAFS fine (0–4 mm)	690	690	550	550
Limestone fines (<1.2 mm)	650	650	900	900
Admixture (% cement weight)	1.5%	1.5%	2%	2%
Total weight (kg)	2815	2805	2725	2715

Table 3
In-fresh mixes properties.

	Slump/Spreading (T_{500} slump flow)	L-box	Fresh Density (Mg/m^3)	Occluded air (%)
IP	165/– mm	–	2.75	2.4
IVP	180/– mm	–	2.69	4.3
ISC	–/680 mm (4.3 sec)	0.87	2.67	1.8
IVSC	–/700 mm (3.8 sec)	0.9	2.57	5.6

or formworks, especially if the target is to produce self-compacting mixtures. The mix gradation and final proportions were finely determined and are shown in Fig. 3 (in volume) and Table 2 (in weight). Preliminary small-scale trials and smaller mass mixes determined the definitive proportions that are reported here [52].

Considering the data displayed in Table 2, it is worth mentioning that cement was in all cases added to the mixes in similar volumetric proportions (about 10.5%) and the water volume of 16–17% was easily deduced. This set of two components constituted around 27% of the total volume of the concrete mixes. The volumetric calculations of the remaining 73% were a priority for managing the workability of mixtures.

In the case of the pumpable mixes, the percentage of EAFS by volume, with regard to the concrete mix, amounted to approximately 50%, in contrast with the limestone fines at 24%. Considering the finer ($\leq$1.2 mm) fraction of EAFS as a part of the cementitious matrix (5%), its theoretical percentage amounted to 27 + 24 + 5 = 56% of the total volume. A correction to account for the occluded air in the cementitious matrix raises that value to 57–58%.

In the self-compacting mixes, the percentage volume of EAFS stood at around 40% in contrast with a limestone fines volume of 33%. The cementitious matrix in theory amounted to 27 + 33 + 4 = 64% and the inclusion of occluded air yielded a value close to 66%. The global in-weight proportion of (EAFS) aggregates with respect to total aggregate weight was 60% in the pumpable mixes and, likewise, 50% in the self-compacting mixes.

The last row of data in Table 2 shows the theoretical in-fresh densities of the concrete mixes. As can be expected, the mixes containing larger amounts of heavy aggregate (EAFS) showed higher densities. Those theoretical values were subsequently experimentally evaluated (see Table 3) and the resultant values turned out to be slightly lower. The presence of occluded air and the inherent difficulty of a highly precise evaluation of the real in-fresh density of the concrete justify the discrepancy.

Each mix (of about one cubic meter) provided sufficient concrete to fill twenty cubic samples of 100 × 100 mm, twenty cylindrical samples of 100 × 200 mm, and ten cylindrical samples of 150 × 300 mm. Additionally, three small prismatic samples (75 × 75 × 285 mm) for the long-term shrinkage tests, were always prepared, plus a few large prismatic samples (150 × 150 × 600 mm) (depending on the remaining surplus from each mix).

3. In-fresh properties of mixtures

An S4 consistency class (slump 160–210 mm) was achieved for the pumpable concretes, IP and IVP; the Abrams cone test values

Please cite this article as: A. Santamaría, V. Ortega-López, M. Skaf et al., The study of properties and behavior of self compacting concrete containing Electric Arc Furnace Slag (EAFS) as aggregate, Ain Shams Engineering Journal, https://doi.org/10.1016/j.asej.2019.10.001

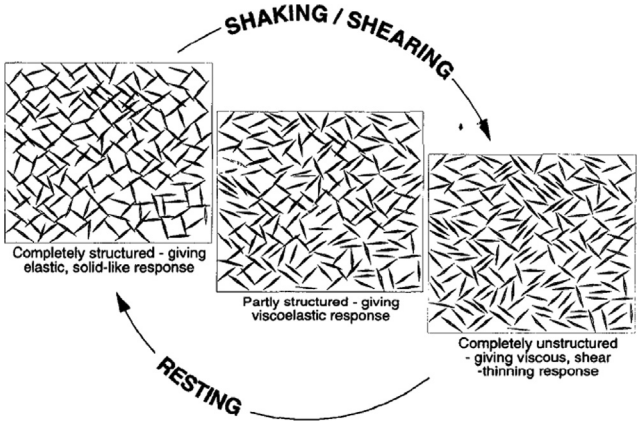

Fig. 4. Thixotropic effect [70].

are presented in Table 3. In this case, the mineral addition in the cement type-IV/B-V (with spherical-vacuolar fly ash particles) slightly increased the short-term concrete workability. Slight vibration of the concrete in the formwork was necessary during the casting processes of the largest pieces.

The amount of occluded air in the IP mix may be considered as "normal" (slightly lower than 3%). In the IVP mixes, the higher amount of occluded air reflected the findings of a previous work by the authors [52].

According to the literature [67,68], the main self-compacting properties of a hydraulic mixture can be specified as mobility, filling ability, and passing ability. Verification of those properties was performed in three tests, although each test was not limited to one single property. The slump test measures the total spread on a plate surface and a 500 mm spread time is used to evaluate both the mobility and the filling ability, while the L-box (triple grill version) test evaluates the capacity of the fluid mass to pass through reinforcement bars.

The results of tests are also shown in Table 3. According to EFNARC guidelines [69], both concretes achieved a SF2 consistency class in the slump flow test, a VS2 class with a spread of 500 mm, and a PA2 class in the L-box test; it must be emphasized that the achievement of these good self-compaction characteristics for large mixtures containing EAFS as aggregate is exceptional and infrequent. The initial workability of the IVSC mix was better than that of the ISC mix, but thixotropic effects were also very evident in the IVSC mix. The self-compacting mixes poured in the formwork required no vibration.

The admixture, a carboxylate-based liquid, acting simultaneously as a water reducer (WR) and viscosity modifier agent (VMA), in general showed good compatibility with the mineral components of concrete, mainly with EAFS. The amount of occluded air, at reasonable levels for all mixes, was slightly lower in the type-I cement mixes, and higher in the type-IV mixes containing fly ash.

3.1. Thixotropic properties of the fresh mixtures

The modeling of the in-fresh mobility of concrete in terms of a Bingham-type plastic material is widely accepted where the initial shear stress of the start and the slope of the flux region are the main variables. The two main admixtures for self-compacting mixes (WR and VMA) act on each of those characteristics. However, the real-life behavior of the concrete mixtures slightly differs from the theoretical model, both due to some singular interactions between the concrete components and due to interactions between the basic concrete components and the chemical admixtures.

The self-compacting concrete manufactured with the type-IV cement was more fluid at first than the one containing the type-I cement, although its workability worsened during the casting process. This worsening was also slightly visible in mixtures made with type-I cement, though much more mitigated. The delayed reduction in workability in the type-IV mixtures can be coarsely and partially explained by slow and progressive water absorption capacities of the mineral active addition (hollow, dusty fly ash), EAF slag, and the fraction of dry limestone fines, although the thixotropic effect is obvious.

Thixotropy is, in our case, defined as a progressive loss of concrete fluidity when the concrete mass is at rest, which is reversible, isothermal, and time-dependent, associated with the interaction between some solid particles influenced by the liquid phase (water modified by admixtures). So, some of our concrete mixtures showed low viscosity when intensely agitated in the industrial mixer, but when poured in the transport ladle and left to rest for some minutes, their fluidity worsened and their filling ability in the formwork was greatly impaired.

As compiled in the extensive work of Barnes [70], Fig. 4 depicts thixotropy as successive states associated with the cement (clinker) particles interacting between each other and with the admixture. The cement particles flocculate, forming a tri-dimensional rigid network (based on the Van-der-Waals forces appearing at the end edges of long particles), when the mass has been left to rest. The network is broken under severe shaking and exposure to shear forces that favor the fluidity of the concrete mass. The authors are convinced that not only the clinker particles, but also the fly-ash and the finest EAFS particles are "active" in this case, due to the severity of the process in the type-IV mixes.

In fact, a very notable loss of workability can be seen in Table 4, in the case of mixtures made with the type-IV cement, which lost most of their fluidity after ten minutes. The "open time" of the type-IV mixtures was really short, complicating the pumping operation and reducing the interval of usefulness of the IVSC mix (by that time, a pumpable mix, despite its initial qualification as a self-compacting mix). In practice, when pumping concrete, the delay between the moment at which the mixer truck stops turning a certain portion, and the moment at which that portion fills the formwork (pumping time) is about five to ten minutes, added to any delay in the pumping system when pouring has to be interrupted, due to work-site organization.

Surprisingly, this negative behavior can to some extent be considered advantageous from the point of view of practical engineering, for mixes IP and ISC, considering that the benefits of concrete stiffening after casting in the molds means that the concrete can be walked upon, decreasing pressure on the formwork and avoiding subsequent segregation of the heavy aggregates. The question is how much control we have over the time extension of the "more fluid period" or "open period". It was tolerable in mixtures based on the type-I cement, but unacceptable in both type-IV mixes. Unfortunately, this aspect of their performance disqualifies these type-IV mixes from practical use as self-compacting mixtures.

3.2. Resistance to segregation

Another practical question relating to the preparation of large batches of concrete is the homogeneity-stability of the whole mass (lack of segregation) when low-viscosity mixes are performed (self-compacting concrete) using EAFS, a particularly heavy aggregate.

In our work, rather than using the prescribed column segregation test (performed on fresh mixes before setting), it was preferred to evaluate segregation in the self-compacting mixtures

Please cite this article as: A. Santamaría, V. Ortega-López, M. Skaf et al., The study of properties and behavior of self compacting concrete containing Electric Arc Furnace Slag (EAFS) as aggregate, Ain Shams Engineering Journal, https://doi.org/10.1016/j.asej.2019.10.001

Table 4
Effects of thixotropy on concrete mixes.

Mix	IP	IVP	ISC	IVSC
Initial Slump/Spreading	165/– mm	180/– mm	–/680 mm	–/700 mm
Slump/Spreading after 10 min	155/– mm	140/– mm	–/620 mm	–/520 mm
Slump/Spreading after 15 min	145/– mm	100/– mm	–/560 mm	–/320 mm

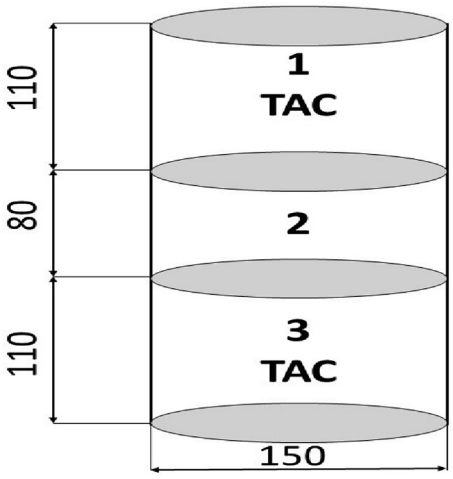

Fig. 5. Cutting a cylindrical specimen to verify segregation.

with an original and direct method instead. When fluid concrete is poured into the formwork, the decantation of heavy EAFS particles can continue for some hours and the conventional test will fail to identify the real situation of the material.

Taking into account the practical nature of this paper on the preparation of large volumes of fairly fluid concrete, the eventual segregation was verified on hardened samples of self-compacting mixtures by CAT (Computerized Axial Tomography), a technique based on X-ray scanning of plane sections and volumetric reconstruction of the internal structures of pieces, used by the authors on similar mixes in previous works [71,72]. The volumetric reconstruction generated different regions colored from light grey to dark grey or even black depending on the average atomic mass of the different particles. Both occluded air and water and heavy EAFS can be distinguished from the cementitious matrix, and the relative volume that each one occupied can be estimated from the total volume.

Two 150 × 300 modeling of the in-fresh mobility of mm cylindrical specimens of each self-compacting mix were employed, due to their similar height with respect to the bending elements manufactured with these mixtures (see Section 5). The samples were cut as shown in Fig. 5 and the resultant upper and lower pieces (labelled as pieces 1 and 3) were tested in the CAT apparatus. The peripheral part of the pieces (10 mm) was discarded, due to the skin effect of concrete that affected the presence of coarse aggregate. Furthermore, the finest fraction of EAFS (smaller than 0.2 mm) cannot be detected due to the pixel resolution. Table 5 displays the results of these measurements. An admissible difference of around 5–6% can be seen in the volumetric fraction of EAFS between the upper and the lower region of the sample.

4. Properties of hardened mixtures

The main mechanical characteristics of the hardened mixtures are presented in Table 6, showing dry densities that varied between 2.52 and 2.71 Mg/m^3. It must be emphasized that the results shown in Table 6 were obtained from cylindrical and cubic samples conserved over one year in a moist chamber (20 °C and at 98% relative humidity).

The evolution of concrete strength is depicted in Fig. 6 after testing cubic samples of 100 × 100 mm; all the mix strengths were at the quality level required for structural concretes. At early ages (until 28 days), the concrete can be divided into two strength classes according to the type of cement that is employed. Concretes manufactured with the type-IV cement reached around 30 MPa and concretes manufactured with the type-I cement were well over 50 MPa. The subsequent evolution of strength in the type-IV cement mixes was clearly influenced by the delayed pozzolanic reaction of fly ash, widely present in that type of cement.

After 360 days of curing in the moist room, the self-compacting concretes reached higher values than those corresponding to the pumpable concretes, for both types of cement, as can be appreciated in Fig. 6. These excellent long-term strengths can be explained by the higher proportion of limestone fines (passing the N°100

Table 5
Volumetric proportions of EAFS in the samples. All data are averages of two measurements.

Mixture Sample	ISC		IVSC	
	Piece 1	Piece 3	Piece 1	Piece 3
EAFS volume (% on total volume)	38.6	40.8	37.9	40.2
Difference between both pieces	5.4%		5.7%	

Table 6
Hardened properties of the mixes.

	Dry density (Mg/m^3)	E (GPa) after 180 days in moist room	Poisson coefficient	Compressive strength 7–28–90–180–360 days in moist room (MPa)	Indirect tensile strength (MPa)	Water penetration depth (mm)	
						Maximum	Average
IP	2.71	38.6	0.23	42–53–63–64–64	5.50	10	7
IVP	2.62	31.4	0.22	18–29–36–48–56	4.45	9	5
ISC	2.60	39.9	0.22	42–53–66–76–77	5.43	19	8
IVSC	2.52	33.8	0.21	19–31–37–55–62	4.62	15	7

Please cite this article as: A. Santamaría, V. Ortega-López, M. Skaf et al., The study of properties and behavior of self compacting concrete containing Electric Arc Furnace Slag (EAFS) as aggregate, Ain Shams Engineering Journal, https://doi.org/10.1016/j.asej.2019.10.001

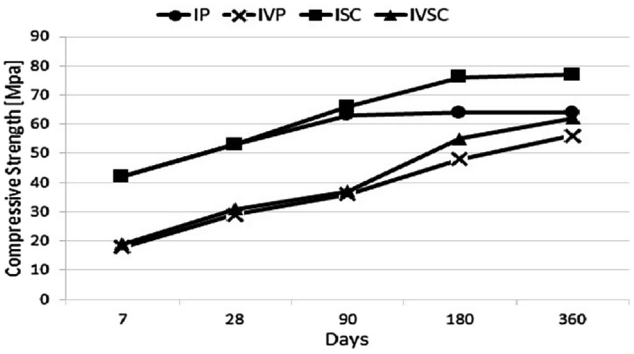

Fig. 6. Development of long-term compressive strength.

ASTM-Tyler sieve [73] with respect to the amount of EAFS in the self-compacting concrete; their presence (up until a certain limit) [74] has also been shown to improve the concrete strength. This affirmation could be justified in Fig. 6 by the increase in strength of the ISC mix (and the IVSC mix where the limestone effect is added to pozzolanic effect) between 90 and 180 days. It seems reasonable to expect that the amount of limestone fines (approximately 240 kg per cubic meter, smaller than 0.15 mm) of the self-compacting mixes (ISC, IVSC) would be close to the ideal content in this "singular" type of concrete containing EAFS aggregate; natural aggregate concretes have lower recommended amounts of fines (160 kg per cubic meter).

The elastic moduli of the concretes manufactured with the type-I cement, measured in cylindrical samples of 150×300 mm, after 180 days of moist room curing, stood at around 40 GPa. The concretes manufactured with the type-IV cement had moduli of 31–34 GPa, as shown in Table 6. The Poisson's moduli values, in all case higher than the "standard" value of 0.2 units, can be attributed to the high proportion of "cementitious matrix" in these mixtures compared with the "conventional" concrete mixtures with only natural aggregates.

Cylindrical samples of 150×300 mm were also tested with conventional methods after 180 days in the moist room to analyze the depth of water penetration under pressure and indirect tensile strength in the Brazilian (splitting) test. In Table 6, mix permeability (fairly similar values) under pressurized water shows a quality range of "low-permeability" concretes, with values lower than the conventional maximum threshold of 25 mm and the average of 15 mm. Likewise, the values obtained for indirect tensile strength (Brazilian test) denoted good quality concrete mixes, with values between 4.45 and 5.5 MPa.

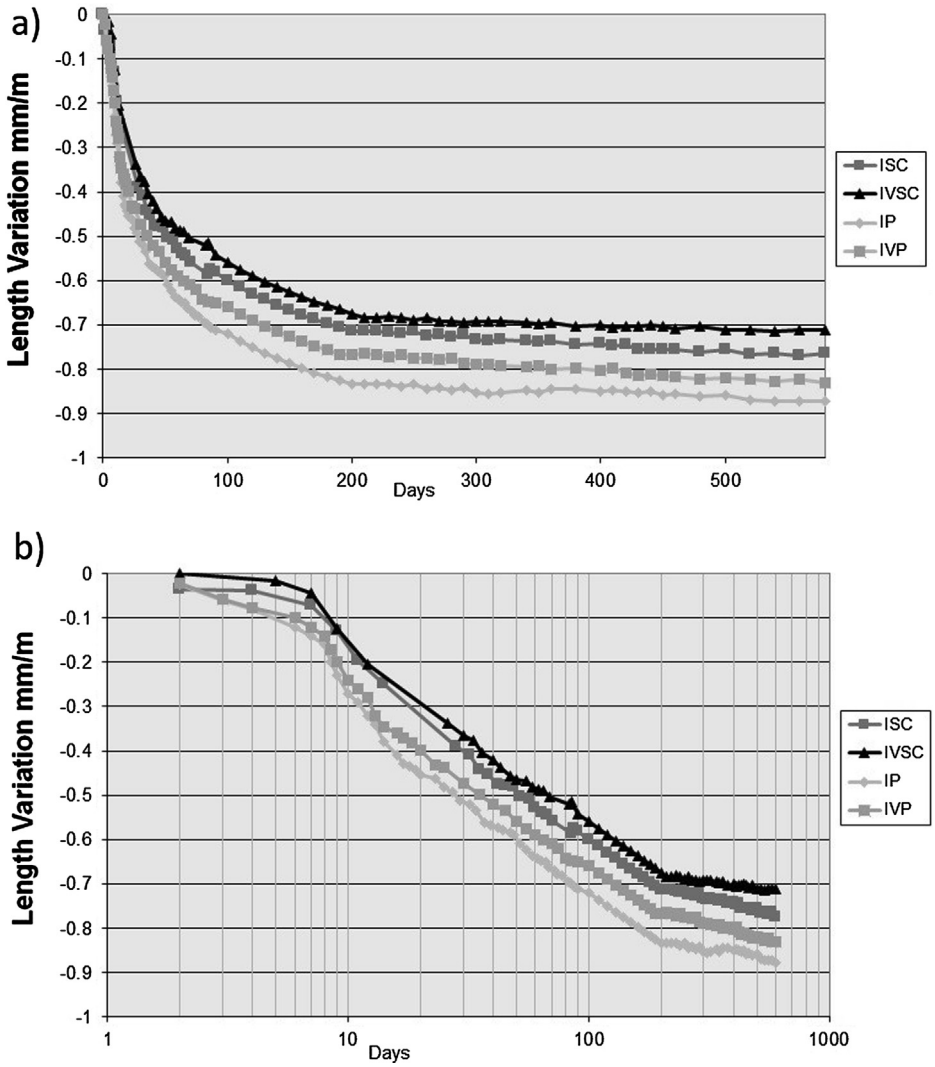

Fig. 7. Shrinkage of EAFS mixtures, 7a linear, 7b logarithmic.

Please cite this article as: A. Santamaría, V. Ortega-López, M. Skaf et al., The study of properties and behavior of self compacting concrete containing Electric Arc Furnace Slag (EAFS) as aggregate, Ain Shams Engineering Journal, https://doi.org/10.1016/j.asej.2019.10.001

Table 7
Capillary test results.

	Final mass (g)	Initial mass (g)	Section (cm^2)	Height (cm)	ε_e (%)	k ($g/m^2 \cdot min^{0.5}$)
IP	2719	2648	100	10	7.1	0.48
IVP	2616	2516	100	10	10	0.68
ISC	2576	2535	100	10	4.1	0.3
IVSC	2547	2493	100	10	5.4	0.37

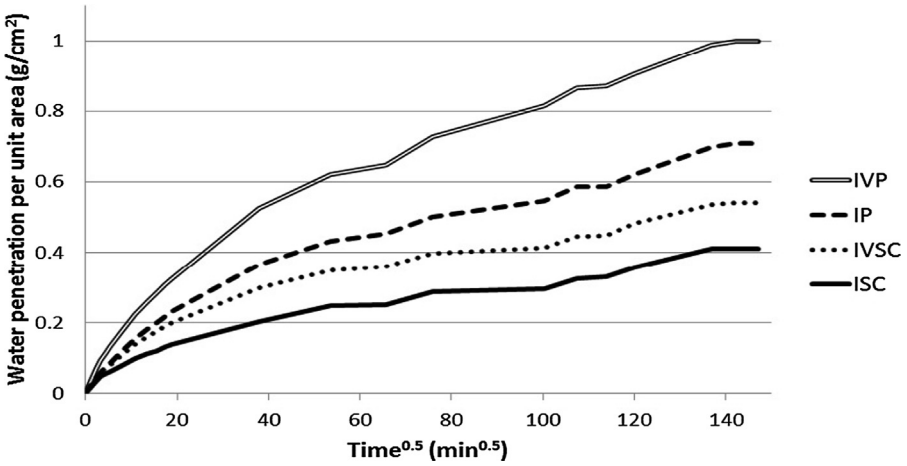

Fig. 8. Water penetration per unit area in grams/cm^2.

4.1. Long-term dry shrinkage

Prismatic specimens sized 75 × 75 × 285mm were used to evaluate the long-term dry shrinkage of the concrete mixes. The elongation over time of three samples of each mix exposed to the indoor environment at room temperature was measured in a rigid frame. The results were expressed as the average of the measurements from three samples.

Fig. 7 depicts the evolution of length variation over time for all mixes with a linear, in 7a, and a logarithmic, in 7b, x-axis. Shrinkage values were globally smaller in the self-compacting mixes than in the pumpable mixes. This tendency, as mentioned in recent works [23,45], confirmed that the pumpable mixes with a high content of EAF slag, in general, showed a slightly higher dry shrinkage than the (self-compacting) mixes containing smaller slag amounts. In contrast, the mixes containing the type-I cement showed slightly higher shrinkage than those containing the type-IV cement, with fly ash; a difference that was consolidated during the first two weeks of curing, in which the hydraulic activity of the type-I cement was very much higher than the pozzolanic reaction of fly ash in the type-IV cement.

Logarithms can be successfully applied to the results for their adjustment over time (x-axis); see Fig. 7b, in which three regions are clearly observed. In the "first region", the logarithmic scale precisely estimated that the above-mentioned period would be between 12 and 14 days in the different mixes. A "second period" from 12 to around 200 days corresponded to the release of "interlayer or inter-crystalline water from binder hydration products", to produce the well-established "long-term dry shrinkage" of the concrete. Very similar sloped curves revealed similar trends in all four mixtures. Finally, a "third period" was noted from about 200 days to the end of the shrinkage test. The graph shows a much flatter slope and in practical terms, the interlayer water was in quasi-equilibrium with the environment, with a very weak loss rate throughout that period.

4.2. Capillary water penetration test

Permeability and porosity tests are usually performed to obtain information on the internal micro-macrostructure of concrete mixes and to establish correlations between microstructure, mechanical behavior, and durability.

The capillarity water penetration test was performed on 100 mm cubic samples conserved in the moist-room and aged 180 days, as per standard UNE 83,982 [75] "Determination of capillarity water absorption of hardened concrete. Fagerlund method"; the test results revealed the capillary structure of the hardened concrete. Based on Darcy's laws of water permeation in porous media, the test constituted an additional verification of the global quality of the mixes, by measuring global porosity, pore-size distribution, connectivity, and even hydrophilicity.

The results are presented in Table 7 using the conventional units (cm, g) of Darcy permeation tests. Following the specifications of the standard, the lower faces of the samples were placed on the bottom of a tray in contact with water, which rises by capillarity from the bottom to the top of the sample. The water supply was constituted by a 10 mm thin layer in the tray, and water was left to permeate (ascend) through a 100 mm high cubic sample by capillary action from the lower face of the sample (scratched face, visible aggregates and matrix, skin effect eliminated) to the upper face. Mass sample gains were evaluated, and the mass gain was plotted against the square root of time, as shown in Fig. 8. The test ended when the water absorption had stabilized and the mass of the saturated sample remained constant over time.

In Table 7, ε_e is the effective porosity of the concrete (measured in this test) and k is the capillary absorption coefficient. The values that were obtained indicated that most of the mixes were of good quality. In fact, effective porosity values of approximately 5% can be qualified as excellent and values of 10% as tolerable. In contrast, capillary absorption values below 1 $g/m^2 \cdot min^{0.5}$ denote very good quality concrete with regard both to strength and to durability.

Please cite this article as: A. Santamaría, V. Ortega-López, M. Skaf et al., The study of properties and behavior of self compacting concrete containing Electric Arc Furnace Slag (EAFS) as aggregate, Ain Shams Engineering Journal, https://doi.org/10.1016/j.asej.2019.10.001

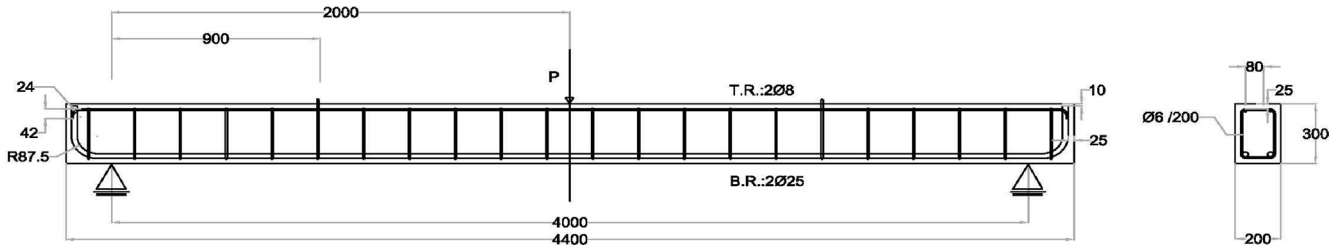

Fig. 9. detail of beam reinforcement in delayed deflection test.

Again, the self-compacting mixtures were of better quality than the pumpable mixes, while mixes IP and ISC showed lower capillary absorption rates than the corresponding mixes IVP and IVSC.

5. Sustained loading testing

Beam-type elements were molded and subsequently tested to support regular in-service loading and to verify the practical performance of these sustainable concrete mixes manufactured in large batches. In the opinion of the authors, this technique is the best way to assess the in-service behavior of elements made with these four types of concrete mixtures. In terms of basic science, this test constitutes an evaluation of the resistance of mixtures against long-term deformation at room temperature, i.e. "room temperature creep". In the literature, no work has been found that performs this test specifically on EAFS self-compacting concrete mixes, although some work has been reported using mixes performed with Construction and Demolition Waste (C&DW) aggregates [76] among others [77,78].

5.1. Specific details of beams and test setup

The nominal dimensions of the molded beams were 200 × 300mm in cross section with a length of 4400 mm. In all, the nominal volume was 0.264 cubic meters, with an approximate weight of around 0.7 Tons. Three beams were molded in each concrete batch and one of them was devoted to this sustained load test. Four reinforced concrete beams (one from each batch) were subjected to long-term deflection tests under sustained loading in a three-point bending test with a clear span of 4 m.

The steel ribbed bars used in the reinforcement were placed as follows: tensile region, bottom, 2Ø25 mm; compressive region, top, 2Ø8 mm, with transversal stirrups of Ø6/200 mm. All the ribbed steel reinforcement bars were included in the class AP 500 S, manufactured with B 500 S steel, as per the specifications in UNE 36,068 standard [75]. The general cover depth of the transversal reinforcing bars was 15 mm; reinforcement details and geometrical characteristics are depicted in Fig. 9.

The test started 180 days after demolding, while the beams were at rest, exposed to an indoor environment in the laboratory test shed. The sustained loading test was performed over a fifteen-month period; it consisted of a first part (one year from 06/21/2016 to 06/22/2017) of deflection under constant loading, and a second part (three months until 09/29/2017) with no external charge (under its own weight), in which the beams partially recovered from the previous deformation.

Three-point bending tests were performed to evaluate the delayed deflection of the beams; the lay out of the test is displayed in Fig. 10. In each beam, an LVDT at the bottom of the midspan section and three classical comparator clocks C1, C2, and C3 on the top face were used to measure all beam displacements, as shown in Fig. 10.

A permanent centered load was applied in the midspan of each beam by means of two hydraulic jacks (yellow) and two steel

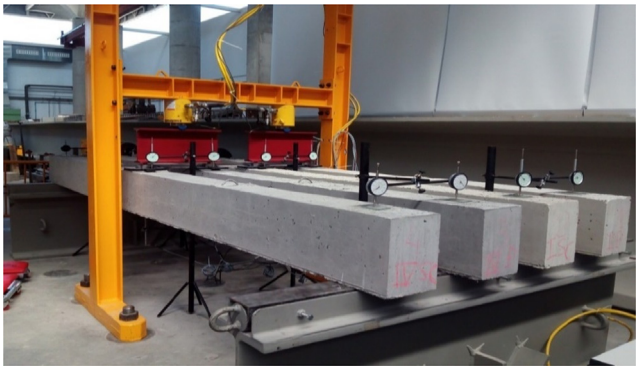

Fig. 10. Lay out of sustained load-delayed deflection test.

pieces for distribution of the load (dark red color in Fig. 10). A load cell on each beam instantaneously transmitted the vertical load values. The load was transferred through two 8 mm thick neoprene plates; the charge level was periodically adjusted with a pump (hydraulic system, manual pump, and a gas-type accumulator), to avoid relaxation greater than 2%.

5.2. Results of long-term deflection under sustained loading test

The beams with a clear span of 4 m were subjected to a sustained concentrated centered surcharge of 40 kN, added to their own weight (section 200 × 300 mm, dry density 2.52 to 2.72 Mg/m^3 as shown in Table 7). That sustained load value was estimated to amount to between one third and one half of the flexural collapse charge, which the authors considered to be representative of the real in-service charge of these reinforced concrete elements. The load level was included in the linear behavior region of the beams in a flexural state (linear ratio between stress and strain in the concrete compressive and steel tensile tests and linear ratio between load and deflection in the whole beam).

The elastic deflections in the central section of the beam after 40 kN initial loading appear in the second column of Table 8 under the heading "initial deflection a(t_o)". The beam deflections after twelve months under sustained loading appear in the third column, under the heading "final deflection a_{360}". The long-term deflections of the IP, ISC, and IVSC-type beams differed (mix IVP was the highest), as can be observed in Fig. 10 in which "t" is a generic instant during the test and a(t), the deflection at any given moment. The use of EAFS in the pumpable and self-compacting mixes yielded the ratio of "total one-year deflection" over "initial deflection", in the order of 1.67 and 1.51 units respectively (fourth column in Table 8). Hence, the experimental "creep deflection ratios" were about 0.67 units in the pumpable mixes and about 0.51 units in the self-compacting mixes.

Finally, the deflection recovery results for instantaneous unloading are shown in the fifth column of Table 8, and the delayed spontaneous unloaded recovery over three months, see Fig. 11

Please cite this article as: A. Santamaría, V. Ortega-López, M. Skaf et al., The study of properties and behavior of self compacting concrete containing Electric Arc Furnace Slag (EAFS) as aggregate, Ain Shams Engineering Journal, https://doi.org/10.1016/j.asej.2019.10.001

Table 8
Long-term deflection test, experimental measures.

	Initial deflection a (t_0) (mm)	Final deflection a_{360} (mm)	Long term (360 days)/initial deflection ratio	Unloading recovery in (mm)	3-month spontaneous recovery in mm	Residual deflection after 15-month (mm)
IP	8.5	14.1	1.65	6.6	0.7	6.8
IVP	10.6	17.8	1.67	8.8	1.1	7.9
ISC	8.4	12.8	1.52	6.3	0.7	5.8
IVSC	8.7	13.2	1.51	7.4	0.8	5.1

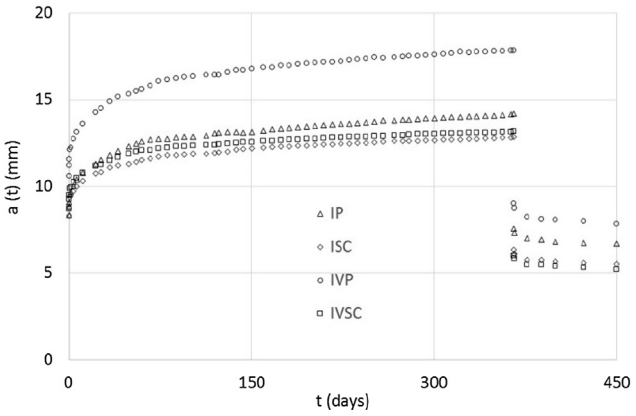

Fig. 11. Deflection of beams over time in the sustained load test.

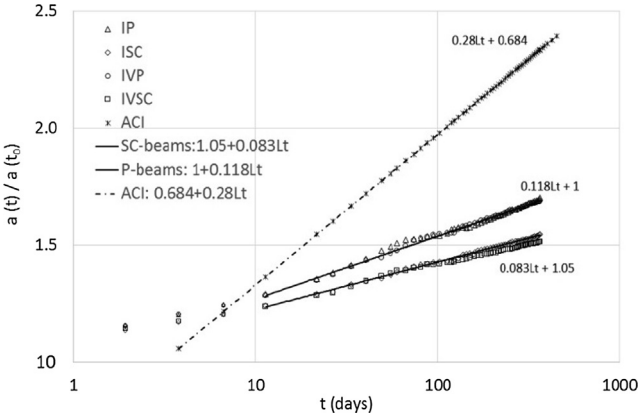

Fig. 12. Relative deflection of beams over time.

from 360 to 450 days, and residual deflection (referring at all times to the central section) are all shown in the final columns of Table 8 (these data are also represented in the ordinates of Fig. 11).

In Fig. 12, the relative deflection (quotient between the total deflection at any moment of the test divided by the initial deflection in each beam) on the y-axis is depicted as a function of time on the x-axis.

The similar specifications for this behavioral test found in the Spanish code EHE-08 [74] and in the ACI 318 code [79], both refer to the lambda coefficient, λ, as the quotient between creep deflection (excluding the initial deflection), at any given moment, divided by the initial post-loading elastic deflection. Furthermore, the equation $\lambda = \xi/(1 + 50\rho_2)$ is also proposed, considering the presence of a light compressive reinforcement $\rho_2 = \frac{A_{s2}}{bd}$; in our case, $\lambda = 0.92 \cdot \xi$.

In Table 9, the values for the "theoretical" coefficient, ξ, are displayed, partially taken from the above-mentioned codes. They represent the long-term creep deflection of any beam (manufactured with an indeterminate concrete) from a large set of historical experimental results. These values of the "theoretical" coefficient, ξ, can be represented by a logarithmic regression as $\xi = 0.304 \cdot Lt - 0.3433$, where time, "t", is measured in days. The values for ξ obtained in our tests on the EAFS concrete beams are also displayed in the two last rows of Table 9; two expressions referred to as "customized formulations" are stated for this function, ξ, deduced from the results of tests performed in this work after a semi-logarithmic regression. As can be seen, the same results were obtained for this coefficient, ξ, in both type-P mixtures, and we obtained the same results in both type-SC mixtures.

In Fig. 12, the different expressions are based on the fact that the magnitude in ordinates represents the total deflection divided by the initial deflection. The ACI 318 code [79] equation for ξ was therefore multiplied by a factor, 0.92, to obtain the lambda value, $\lambda = 0.28 \cdot Lt - 0.316$, and when a unit is added, the ratio $a(t)/a(t_o) = 1 + \lambda = 0.28 \cdot Lt + 0.684$. The expressions displayed in Fig. 12 for the $a(t)/a(t_o)$ factor in the P-beams and SC-beams, derived from the experimental results after a linear regression in logarithmic scale, were calculated in the same way from the "customized formulations" shown in Table 9.

The deflection predictions after 360 days in EHE-08 [74] and ACI 318 [79], see Table 9, are based on the results of concretes made with (standard) aggregates and components, which yielded a figure of 1.45 units in terms of the ξ coefficient; a much higher value than 0.58–0.76 units obtained for ξ after regression in our beams. In rows 5 and 6 of Table 9, the ratios (in percentage terms) of the experimental results with respect to the theoretical values specified in the standards (row 4) are displayed; in the long-term (5 years), those values are close to 50% in the pumpable mixes and 38% in the self-compacting mixes.

Customized formulations:

$$\xi = 0.13\hat{A} \cdot Ln(t) + 0.001 (for\ \ beam\ \ type\ \ P);$$

$$\xi = 0.09\hat{A} \cdot Ln(t) + 0.054 (for\ \ beam\ \ type\ \ SC)$$

Table 9
Theoretical and experimental results of beam deflection (percentages between brackets).

Days	7	30	60	90	180	240	300	360	730	1095	1460	1825
Months	0.2	1	2	3	6	8	10	12	24	36	48	60
Years	0.0	0.1	0.2	0.2	0.5	0.7	0.8	1	2	3	4	5
ξ theoretical	0.25	0.69	0.90	1.0	1.2	1.32	1.39	1.45	1.66	1.78	1.87	1.94
ξ beams P (%)	0.25 (100)	0.43 (62))	0.52 (58)	0.57 (57)	0.65 (54)	0.69 (52)	0.72 (52)	0.76 (52)	0.85 (51)	0.9 (51)	0.94 (50)	0.97 (50)
ξ beams SC (%)	0.23 (92)	0.36 (52)	0.42 (47)	0.46 (46)	0.52 (43)	0.55 (42)	0.57 (41)	0.58 (40)	0.65 (39)	0.68 (38)	0.71 (38)	0.73 (38)

Please cite this article as: A. Santamaría, V. Ortega-López, M. Skaf et al., The study of properties and behavior of self compacting concrete containing Electric Arc Furnace Slag (EAFS) as aggregate, Ain Shams Engineering Journal, https://doi.org/10.1016/j.asej.2019.10.001

It can be observed that our experimental values are about one half or three-fifths of the value proposed by the aforementioned calculation codes, although the EAFS aggregate could not be mentioned as the only cause. The code predictions recorded far higher values, probably because the calculation codes include the "addition" of the two experimental effects affecting the dimensional stability of concrete, creep, and shrinkage. Logically, the deflections in our tests are thought to be mainly due to the creep effect, while the influence of shrinkage was probably minor or negligible, due to the initial rest state of the beams over six months, previous to the loading of these tests, as mentioned in Section 5.1.

The most relevant observation following these long-term tests on four mixtures is the difference in the long-term behavior between the type-P (pumpable) and the type-SC (self-compacting) mixtures, both of which were independent of the cement type. The self-compacting mixes showed a much better behavior than the corresponding pumpable mixes in view of the long-term deformation under constant loading (creep at room temperature), and their most relevant differential characteristic, as previously mentioned, was the larger amount of suitably sized limestone fines in the self-compacting rather than in the pumpable mixtures. The positive features of permeability (see Table 7) and porosity of the self-compacting mixes, lower than that of the corresponding pumpable mixes (better pore sizing to resist creep and better compactness in SC mixes) were considered decisive factors on that question. The results of other authors [80] agree with these values using recycled and natural aggregates and large volumes of fly ash, as in our study on the type-IV cement mixtures.

It can finally be concluded that a massive use of EAFS as aggregate in the concrete mixtures showed no detrimental long-term characteristics (and could even be qualified as fairly good), in comparison with an "average" broad set of results for conventional aggregate mixtures following the same standard specifications and calculation codes.

6. Conclusions

The main conclusions of this study can be summarized as follows.

- Two self-compacting concrete mixtures and two pumpable concrete mixtures containing high amounts of EAFS aggregate and using two different Portland cements (types I and IV) have been successfully designed and manufactured in batches of one cubic meter by volume. Consistency classes of S4 and SF2 were achieved in the slump tests for the pumpable and the self-compacting mixes, respectively.
- Self-compacting mixtures initially showed fairly good properties in the fresh state, for filling formworks with a steel reinforcement cage, when submitted to classical flowability and stability tests (spreading close to 700 mm, T_{500} close to 4 sec, L-box value 0.9 units, and segregation less than 6%).
- Undesirable thixotropic effects were detected in both the self-compacting and the pumpable mixes made with the type-IV Portland cement. Any chance of using this kind of cement in large volumes of concrete is therefore limited.
- The mechanical and the dimensional characteristics of the mixes used in this work (compressive and tensile strength, stiffness, long-term shrinkage), obtained on samples conserved in moist room, denoted good quality concretes, useful for the production of reliable and durable construction and building elements.
- The internal concrete microstructure, evaluated by means of water penetration under pressure tests, and capillary absorption of water tests performed on laboratory samples from moist room, was in general fairly good, mainly in self-compacting mixes.
- The resistance to sustained load of flexural elements made with these mixtures can be grouped into two categories. Relative deflection (creep deflection of beams divided by the initial instantaneous deflection) of the pumpable mixes was greater than the relative deflection of the self-compacting mixes (about 52% of the maximum value proposed by conventional standards in the case of pumpable mixes, and about 40% in the case of self-compacting mixes); the quality of the self-compacting EAFS concrete mixtures was excellent at withstanding sustained loading.

Declaration of Competing Interest

None

Acknowledgements

The authors wish to express their gratitude to: the Vice-Rectorate of Investigation of the University of the Basque Country (UPV/EHU) [PIF 2013]; the Vice-Rectorate of Investigation of the University of Burgos [SUCONS]; the Junta de Castilla y León (Regional Government) for funding the UIC-231 group through project BU119P17 partially supported by FEDER funds; Project RTI2018-097079-B-C31 (MCIU/AEI/EU) and the UPV/EHU [PPGA19/61]. Moreover, we are also grateful to both the Basque Government research group (IT1314-19) and the companies Chryso Additives and Hormor-Zestoa for their ongoing collaboration with the present research group.

References

[1] Malhotra V. SP-202: third Canmet/ACI International Symposium: sustaibable development of cement and concrete. ACI Spl Publ 2001;202:490.
[2] Faleschini F, De Marzi P, Pellegrino C. Recycled concrete containing EAF slag: environmental assessment through LCA. Eur J Environ Civ Eng 2014;18 (9):1009–24. https://doi.org/10.1080/19648189.2014.922505.
[3] Pellegrino C, Faleschini F. Sustainability improvements in the concrete industry: use of recycled materials for structural concrete production. In: Green energy and technology serie. Springer; 2016. https://doi.org/10.1007/978-3-319-28540-5.
[4] Qasrawi H. The use of steel slag aggregate to enhance the mechanical properties of recycled aggregate concrete and retain the environment. Constr Build Mater 2014;54:298–304. https://doi.org/10.1016/j.conbuildmat.2013.12.063.
[5] Sofi A. Effect of waste tyre rubber on mechanical and durability properties of concrete – a review. Ain Shams Eng J 2018;9(4):2691–700. https://doi.org/10.1016/j.asej.2017.08.007.
[6] Chowdhury S, Mishra M, Suganya O. The incorporation of wood waste ash as a partial cement replacement material for making structural grade concrete: an overview. Ain Shams Eng J 2015;6(2):429–37. https://doi.org/10.1016/j.asej.2014.11.005.
[7] Ghrair AM, Al-Mashaqbeh OA, Sarireh MK, Al-Kouz N, Farfoura M, Megdal SB. Influence of grey water on physical and mechanical properties of mortar and concrete mixes. Ain Shams Eng J 2018;9(4):1519–25. https://doi.org/10.1016/j.asej.2016.11.005.
[8] Phanikumar BR, Sofi A. Effect of pond ash and steel fibre on engineering properties of concrete. Ain Shams Eng J 2016;7(1):89–99. https://doi.org/10.1016/j.asej.2015.03.009.
[9] Mohamed HA. Effect of fly ash and silica fume on compressive strength of self-compacting concrete under different curing conditions. Ain Shams Eng J 2011;2(2):79–86. https://doi.org/10.1016/j.asej.2011.06.001.
[10] Bosela P, Delatte N, Obratil R, Patel A. Fresh and hardened properties of paving concrete with steel slag aggregate. Propiedades para firmes del hormigón fabricado con áridos siderúrgicos. Revista técnica de la Asociación Española de la Carretera 2009;4(166):55–66.
[11] Rubio AR, Carretero JG. La aplicación de las escorias de acería en Carreteras. Ing Civ 1991;80:5–9.
[12] Ebrahim Abu El-Maaty Behiry A. Utilization of cement treated recycled concrete aggregates as base or subbase layer in Egypt. Ain Shams Eng J 2013;4 (4):661–73. https://doi.org/10.1016/j.asej.2013.02.005.
[13] Roy S, Miura T, Nakamura H, Yamamoto Y. Investigation on applicability of spherical shaped EAF slag fine aggregate in pavement concrete – fundamental and durability properties. Constr Build Mater 2018;192:555–68. https://doi.org/10.1016/j.conbuildmat.2018.10.157.

[14] Huseien GF, Mirza J, Ismail M, Ghoshal SK, Ariffin MAM. Effect of metakaolin replaced granulated blast furnace slag on fresh and early strength properties of geopolymer mortar. Ain Shams Eng J 2018;9(4):1557–66. https://doi.org/10.1016/j.asej.2016.11.011.
[15] Skaf M, Manso JM, Aragón Á, Fuente-Alonso JA, Ortega-López V. EAF slag in asphalt mixes: a brief review of its possible re-use. Resour Conserv Recycl 2017;120:176–85. https://doi.org/10.1016/j.resconrec.2016.12.009.
[16] Pasetto M, Baldo N. Experimental evaluation of high performance base course and road base asphalt concrete with electric arc furnace steel slags. J Haz Mater 2010;181(1–3):938–48. https://doi.org/10.1016/j.jhazmat.2010.05.104.
[17] Pasetto M, Baldo N. Fatigue behavior characterization of bituminous mixtures made with reclaimed asphalt pavement and steel slag. Procedia-Soc Behav Sci 2012:297–306.
[18] Pasetto M, Baldo N. Mix design and performance analysis of asphalt concretes with electric arc furnace slag. Constr Build Mater 2011;25(8):3458–68. https://doi.org/10.1016/j.conbuildmat.2011.03.037.
[19] San José JT, Uría A. Escorias de horno de arco eléctrico en mezclas bituminosas. Arte y Cemento 2001;1905:122–5.
[20] Yildirim IZ, Prezzi M. Use of steel slag in subgrade applications, publication FWA/IN/JTRP-2009/32. Joint transportation research program. West Lafayette (IN): Indiana Department of Transportation and Purdue University; 2009.
[21] Behiry AEAEM. Evaluation of steel slag and crushed limestone mixtures as subbase material in flexible pavement. Ain Shams Eng J 2013;4(1):43–53. https://doi.org/10.1016/j.asej.2012.07.006.
[22] Skaf M, Ortega-Lopez V, Fuente-Alonso JA, Santamaria A, Manso JM. Ladle furnace slag in asphalt mixes. Constr Build Mater 2016;122:488–95. https://doi.org/10.1016/j.conbuildmat.2016.06.085.
[23] Santamaría A, Rojí E, Skaf M, Marcos I, González JJ. The use of steelmaking slags and fly ash in structural mortars. Constr Build Mater 2016;106:364–73. https://doi.org/10.1016/j.conbuildmat.2015.12.121.
[24] Al-Negheimish AI, Al-Zaid RZ. Utilization of local steel making slag in concrete. J King Saud Univ 1997;9(1):39–55.
[25] Fronek B, Bosela P, Delatte N. Steel slag aggregate used in portland cement concrete. Transp Res Rec 2012:37–42.
[26] Manso JM, Hernández D, Losáñez MM, González JJ. Design and elaboration of concrete mixtures using steelmaking slags. ACI Mater J 2011;108(6):673–81.
[27] Manso JM, Gonzalez JJ, Polanco JA. Electric arc furnace slag in concrete. J Mater Civil Eng 2004;16(6):639–45. https://doi.org/10.1061/(ASCE)0899-1561(2004)16:6(639).
[28] Shekarchi M, Soltani M, Alizadeh R, Chini M, Ghods P, Hoseini M, et al. Study of the mechanical properties of heavy weight preplaced aggregate concrete using electric arc furnace slag as aggregate. International conference on concrete engineering and technology, Malaysia, 2004.
[29] Faleschini F, Zanini MA, Pellegrino C. New perspectives in the use of electric arc furnace slag as coarse aggregate for structural concrete. International conference Euroslag, Linz, Austria, 2015.
[30] Cho BS, Choi YC. Hydration properties of STS-refining slag-blended blast furnace slag cement. Adv Mater Sci Eng 2018:. https://doi.org/10.1155/2018/58932545893254.
[31] Cho BS, Choi YC. Properties of cementless binders using desulfurization slag as an alkali activator. J Ceram Process Res 2018;19(1):37–42.
[32] Morino K, Iwatsuki E. Utilization of electric arc furnace oxidizing slag. In: Gaballah I, Hager J, Solozabal R, editors. Minerals, metals and materials society/AIME, REWAS'99: Global Symposium on Recycling. San Sebastian: Waste Treatment and Clean Technology; 1999. p. 521–30.
[33] López FA, López-Delgado A, Balcázar N. Physico-chemical and mineralogical properties of EAF and AOD Slags. Afinidad LIII 1996;53(461):39–46.
[34] Yildirim IZ, Prezzi M. Chemical, mineralogical, and morphological properties of steel slag. Adv Civ Eng 2011. https://doi.org/10.1155/2011/463638.
[35] Jiang Y, Ling TC, Shi C, Pan SY. Characteristics of steel slags and their use in cement and concrete—a review. Resour Conserv Recycl 2018;136:187–97. https://doi.org/10.1016/j.resconrec.2018.04.023.
[36] Elkoumy MM, El-Anwar M, Fathy AM, Megahed GM, El-Mahallawi I, Ahmed H. Simulation of EAF refining stage. Ain Shams Eng J 2018;9(4):2781–93. https://doi.org/10.1016/j.asej.2017.10.002.
[37] Manso JM, Setién J. Investigación de nuevos usos de las escorias de horno eléctrico de arco (EAF): la oportunidad de los hormigones. Hormigón y acero 2006;241:51–7.
[38] Etxeberria M, Pacheco C, Meneses JM, Berridi I. Properties of concrete using metallurgical industrial by-products as aggregates. Constr Build Mater 2010;24(9):1594–600. https://doi.org/10.1016/j.conbuildmat.2010.02.034.
[39] Abu-Eishah SI, El-Dieb AS, Bedir MS. Performance of concrete mixtures made with electric arc furnace (EAF) steel slag aggregate produced in the Arabian Gulf region. Constr Build Mater 2012;34:249–56. https://doi.org/10.1016/j.conbuildmat.2012.02.012.
[40] Monosi S, Ruello ML, Sani D. Electric arc furnace slag as natural aggregate replacement in concrete production. Cem Concr Compos 2016;66:66–72. https://doi.org/10.1016/j.cemconcomp.2015.10.004.
[41] Pellegrino C, Cavagnis P, Faleschini F, Brunelli K. Properties of concretes with black/oxidizing electric arc furnace slag aggregate. Cem Concr Compos 2013;37(1):232–40. https://doi.org/10.1016/j.cemconcomp.2012.09.001.
[42] Pellegrino C, Gaddo V. Mechanical and durability characteristics of concrete containing EAF slag as aggregate. Cem Concr Compos 2009;31(9):663–71. https://doi.org/10.1016/j.cemconcomp.2009.05.006.
[43] Papayianni I, Anastasiou E. Production of high-strength concrete using high volume of industrial by-products. Constr Build Mater 2010;24(8):1412–7. https://doi.org/10.1016/j.conbuildmat.2010.01.016.
[44] Polanco JA, Manso JM, Setién J, González JJ. Strength and durability of concrete made with electric steelmaking slag. ACI Mater J 2011;108(2):196–203.
[45] Arribas I, Vegas I, San-José JT, Manso JM. Durability studies on steelmaking slag concretes. Mater Des 2014;63:168–76. https://doi.org/10.1016/j.matdes.2014.06.002.
[46] Manso JM, Polanco JA, Losañez M, González JJ. Durability of concrete made with EAF slag as aggregate. Cem Concr Compos 2006;28(6):528–34. https://doi.org/10.1016/j.cemconcomp.2006.02.008.
[47] Faleschini F, Alejandro Fernández-Ruíz M, Zanini MA, Brunelli K, Pellegrino C, Hernández-Montes E. High performance concrete with electric arc furnace slag as aggregate: mechanical and durability properties. Constr Build Mater 2015;101:113–21. https://doi.org/10.1016/j.conbuildmat.2015.10.022.
[48] Santamaría A, Orbe A, San José JT, González JJ. A study on the durability of structural concrete incorporating electric steelmaking slags. Constr Build Mater 2018;161:94–111. https://doi.org/10.1016/j.conbuildmat.2017.11.121.
[49] González-Ortega MA, Cavalaro SHP, Rodríguez de Sensale G, Aguado A. Durability of concrete with electric arc furnace slag aggregate. Constr Build Mater 2019;217:543–56. https://doi.org/10.1016/j.conbuildmat.2019.05.082.
[50] García Mochales JL. Utilización de áridos siderúrgicos en obras por la autoridad portuaria de Bilbao; 2016.
[51] Zanini MA. Structural reliability of bridges realized with reinforced concretes containing electric arc furnace slag aggregates. Eng Struct 2019;188:305–19. https://doi.org/10.1016/j.engstruct.2019.02.052.
[52] Santamaría A, Orbe A, Losañez MM, Skaf M, Ortega-Lopez V, González JJ. Self-compacting concrete incorporating electric arc-furnace steelmaking slag as aggregate. Mater Des 2017;115:179–93. https://doi.org/10.1016/j.matdes.2016.11.048.
[53] Fuente-Alonso JA, Ortega-López V, Skaf M, Aragón A, San-José JT. Performance of fiber-reinforced eaf slag concrete for use in pavements. Constr Build Mater 2017;149:629–38. https://doi.org/10.1016/j.conbuildmat.2017.05.174.
[54] Ortega-López V, Fuente-Alonso JA, Santamaría A, San-José JT, Aragón Á. Durability studies on fiber-reinforced EAF slag concrete for pavements. Constr Build Mater 2018;163:471–81. https://doi.org/10.1016/j.conbuildmat.2017.12.121.
[55] Qasrawi H. Towards sustainable self-compacting concrete: effect of recycled slag coarse aggregate on the fresh properties of SCC. Adv Civ Eng 2018;2018. https://doi.org/10.1155/2018/7450943.
[56] Qasrawi H. Fresh properties of green SCC made with recycled steel slag coarse aggregate under normal and hot weather. J Clean Prod 2018;204:980–91. https://doi.org/10.1016/j.jclepro.2018.09.075.
[57] Kim SW, Lee YJ, Kim KH. Flexural behavior of reinforced concrete beams with electric arc furnace slag aggregates. J Asian Archit Build Eng 2012;11(1):133–8. https://doi.org/10.3130/jaabe.11.133.
[58] Kim S-W, Lee Y-J, Lee Y-H, Kim K-H. Flexural Performance of reinforced high-strength concrete beams with EAF oxidizing slag aggregates. J Asian Archit Build Eng 2016;15(3):589–96. https://doi.org/10.3130/jaabe.15.589.
[59] Lee YJ, Kim HG, Park JH, Lee KS, Kim KH. Flexural behaviour prediction for RC beams in consideration of compressive stress distribution of concrete with electric arc furnace oxidising slag aggregates. Eur J Environ Civ Eng 2017:1–20. https://doi.org/10.1080/19648189.2017.1417916.
[60] Kim SW, Lee YJ, Kim KH. Bond behavior of RC beams with electric arc furnace oxidizing slag aggregates. J Asian Archit Build Eng 2012;11(2):359–66. https://doi.org/10.3130/jaabe.11.359.
[61] Pellegrino C, Faleschini F. Experimental behavior of reinforced concrete beams with electric arc furnace slag as recycled aggregate. ACI Mater J 2013;110(2):197–205.
[62] Faleschini F, Santamaria A, Zanini MA, San José JT, Pellegrino C. Bond between steel reinforcement bars and electric arc furnace slag concrete. Mater Struct 2017;50(3). https://doi.org/10.1617/s11527-017-1038-2.
[63] Faleschini F, Hofer L, Zanini MA, dalla Benetta M, Pellegrino C. Experimental behavior of beam-column joints made with EAF concrete under cyclic loading. Eng Struc 2017;139:81–95. https://doi.org/10.1016/j.engstruct.2017.02.038.
[64] Pellegrino C, Faleschini F. Experimental investigation on RC beams containing slag as recycled aggregate, fib Symposium 2012. Stockholm: Concrete Structures for Sustainable Community; 2012. p. 451–4.
[65] CEN. European Committee for Standardization. Rue de Stassart, 36. Brussels B-1050.
[66] Penteado CSG, Evangelista BL, Ferreira GCdS, Borges PHA, Lintz RCC. Use of electric arc furnace slag for producing concrete paving blocks. 2019;19(2):21–32. https://doi.org//10.1590/s1678-86212019000200305.
[67] Okamura H. Self-compacting high-performance concrete. Concr Int 1997;19(7):50–4.
[68] Okamura H, Ouchi M. Self-compacting concrete. J Adv Concr Technol 2003;1(1):5–15.
[69] EFNARC. Specification guidelines for self-compacting concrete. European Federation of Producers and Applicators of Specialist Products for Structures; 2002.
[70] Barnes HA. Thixotropy – a general review. J Non-Newton Fluid Mech 1997;70:1–33.
[71] Manso JM, Rodriguez A, Aragón A, Gonzalez JJ. The durability of masonry mortars made with ladle furnace slag. Constr Build Mater 2011;25(8):3508–19. https://doi.org/10.1016/j.conbuildmat.2011.03.044.

Please cite this article as: A. Santamaría, V. Ortega-López, M. Skaf et al., The study of properties and behavior of self compacting concrete containing Electric Arc Furnace Slag (EAFS) as aggregate, Ain Shams Engineering Journal, https://doi.org/10.1016/j.asej.2019.10.001

[72] Santamaría A, Ortega-López V, Skaf M, Marcos I, San-José J-T, González JJ. Performance of hydraulic mixes manufactured with electric arc furnace slag aggregates. In: Meyers MA, editor. Proceedings of the 3rd Pan American Materials Congress. Cham: Springer International Publishing; 2017. p. 227–34.
[73] Annual Book of ASTM Standars. West Conshohocken (PA), USA: ASTM International; 2008.
[74] EHE 08. Concrete Standard/Instrucción de Hormigón Estructural, Ministerio de Fomento. Gobierno de España. Madrid: Secretaria General Técnica; 2008.
[75] UNE Spanish Standars. AENOR, Madrid, Spain.
[76] Fiol F, Thomas C, Muñoz C, Ortega-López V, Manso JM. The influence of recycled aggregates from precast elements on the mechanical properties of structural self-compacting concrete. Constr Build Mater 2018;182:309–23. https://doi.org/10.1016/j.conbuildmat.2018.06.132.
[77] Mohamed HA. Effect of using swimmer bars on the behavior of normal and high strength reinforced concrete beams. Ain Shams Eng J 2017;8(1):29–37. https://doi.org/10.1016/j.asej.2015.07.007.
[78] Sofi A, Phanikumar BR. An experimental investigation on flexural behaviour of fibre-reinforced pond ash-modified concrete. Ain Shams Eng J 2015;6(4):1133–42. https://doi.org/10.1016/j.asej.2015.03.008.
[79] ACI Committee 318M-14 y RM-14. Building code requirements for structural concrete: Farmington Hills, MI: American Concrete Institute.
[80] Tošić N, Marinković S, Pecić N, Ignjatović I, Dragaš J. Long-term behaviour of reinforced beams made with natural or recycled aggregate concrete and high-volume fly ash concrete. Constr Build Mater 2018;176:344–58. https://doi.org/10.1016/j.conbuildmat.2018.05.002.

Dr. Amaia Santamaría PhD. in Civil Engineering from the University of the Basque Country. She holds a Master in Construction Engineering. Currently, she occupies a position at the University of Basque Country in the Area of Continuous Media Mechanics and Structures. She has developed an international doctorate focused on the reuse of steelmaking slag in the construction sector. She has published 12 scientific papers (WOS indexed), 9 Q1; 11 papers in 8 international congresses being 1 of them indexed and took part in 6 different scientific events. She has participated in 2 R&D projects and actually she is involved in 4 different R&D projects.

Dr. Vanesa Ortega-López PhD. in Civil and Industrial Engineering from the University of Burgos. She is Associate Professor in the Area of Continuous Media Mechanics and Structures of the University of Burgos. Member of the SUCONS (Sustainable Construction Research Group) and member of the Consolidated Research Unit UIC-231 of the JCyL (Regional Government). Co-author of 15 articles (11Q1), indexed in JCR (WoS), 2 book chapters, 3 patents and 20 publications in conference proceedings. She has participated in 6 competitive R&D Projects and 6 contracts with companies, mostly related to investigations in new materials, structures and reuse of waste in construction.

Dr. Marta Skaf Ph.D in the University of Burgos and MEng. Civil Engineer in the University of Cantabria. Assistant Professor at the University of Burgos in the Department of Construction, teaching mainly in the Civil Engineering Bacheloŕs Degree. She belongs to the Sustainable Construction Research Group and her current research work focuses on construction materials with steel slags: two competitive R&D Projects, several research projects and contracts with companies, 6 JCR articles published, many communications in International Conferences and three Patents granted in that field.

Dr. José A. Chica MSc. in Mechanical Engineer from the University of the Basque Country and PhD. in Structural and Mechanical Engineering from the University of Burgos. He holds an Executive MBA, an International Executive Programme from Georgetown University and he is currently studying for an Executive Certificate on Strategy and Innovation at the Massachusetts Institute of Technology - Sloan School of Management. Director for Digital Construction in TECNALIA and member of the Technical Group for the monitoring of the Research Fund for Coal and Steel. He was also member of the European Steel Technology Platform and of the Eurocode Evolution Groups.

Dr. Juan Manuel Manso Full Professor at the University Burgos and Vice-Chancellor of Planning, Services and Sustainability. Within the SUCONS group, he holds 22 articles indexed in JCR, three books, four patents, more than 30 International Conferences and several Thesis directed, mainly related to the reuse of waste in construction materials. He has participated in 22 research projects and/or contracts, being coordinator of three important R&D competitive projects at National and European levels. International expert and avisor, member of numerous Scientific Committees.

Please cite this article as: A. Santamaría, V. Ortega-López, M. Skaf et al., The study of properties and behavior of self compacting concrete containing Electric Arc Furnace Slag (EAFS) as aggregate, Ain Shams Engineering Journal, https://doi.org/10.1016/j.asej.2019.10.001